

Electron Transfer Kinetics of Tris(1,10-phenanthroline)ruthenium(II) Electrooxidation in Aprotic Solvents

Krzysztof Winkler,[‡] Novelette McKnight,^{†,§} and W. Ronald Fawcett^{*,†}

Department of Chemistry, University of California, Davis, California 95616 and Institute of Chemistry, University of Białystok, 15443 Białystok, Poland

Received: October 5, 1999; In Final Form: January 21, 2000

Double layer and solvent effects on the kinetics of the one-electron oxidation of $\text{Ru}(\text{phen})_3^{2+}$ (where phen = 1,10-phenanthroline) at platinum and gold ultramicroelectrodes were studied by ac-voltammetry. The standard rate constant of $\text{Ru}(\text{phen})_3^{2+}$ electrooxidation is independent of both electrode material and concentration of supporting electrolyte, indicating the absence of double-layer effects on the kinetics of electron transfer. The small variation of the formal redox potential of the $\text{Ru}(\text{phen})_3^{2+/3+}$ system with change of the supporting electrolyte concentration demonstrates the absence of a significant influence of ion pairing on the reaction rate. Therefore, the electrode process of $\text{Ru}(\text{phen})_3^{2+}$ oxidation is found to be ideally suitable for the study of solvent effects on electron transfer kinetics. The solvent dependence of the electron transfer rate constant was interpreted within the context of contemporary theory. The charge transfer process was found to be perfectly adiabatic. Since the crossing rate of the energy barrier is controlled by the dynamics of solvent relaxation, the rate of the electrode reaction primarily depends on the solvent's longitudinal relaxation time or, more approximately, on the viscosity of the solution.

Introduction

Considerable attention has been paid to electrochemistry involving polyimine (2,2'-bipyridine (bpy), 1,10-phenanthroline (phen), 2,2',2''-terpyridine (terpy), 2,2'-bipyrazine (bpyz)) complexes of ruthenium(II) for both fundamental and applied reasons. In these compounds, metal-centered and ligand-centered electron-transfer processes occur in two distinct potential regions.^{1–5} The most extensively studied $\text{Ru}(\text{bpy})_3^{2+}$ complex exhibits a one-electron metal-centered oxidation process in the positive potential range. At negative potentials, this complex undergoes up to six successive reversible one-electron reduction steps, which are related to the reduction of the bpy ligands.^{1,2} Similar electrochemical behavior has been reported for other polyimine analogues of ruthenium (II).¹ The $\text{Ru}(\text{L})_3^{2+/3+}$ (where L is the diimine ligand) redox system has been used to study the relationship between the spectroscopic and electrochemical properties of these complexes.¹ There has also been considerable interest in electroactive polymers incorporating ruthenium(II) polypyridyl systems.^{6–8} These systems can be used as electronic devices,^{9–11} electron-transfer mediators,^{8,12,13} or electroanalytical sensors.¹⁴ The photophysical properties of polypyridyl ruthenium(II) complexes have also received much scrutiny because of their potential as photosensitizers for electron-transfer processes.^{15–18}

While there have been a number of thermodynamic studies of electrode processes of $\text{Ru}(\text{L})_3^{2+}$, little is known about the kinetics of these electron-transfer reactions. Saji and Aoyagui¹⁹ studied the kinetics of the ligand-centered reduction processes of tris(2,2'-bipyridine) ruthenium(II) complexes. They observed a correlation between the electron-transfer rate and the changes of electronic configuration of the reactant during the electron-

transfer step. The observed standard rate constants (k_s) were close to 0.2 cm s^{-1} . The kinetics of the oxidation of polyimine complexes of ruthenium(II) has not been investigated until now.

In this paper, we report kinetic data obtained by the high-frequency ac-admittance technique for the electrooxidation of $\text{Ru}(\text{phen})_3^{2+}$ in a variety of solvents. One of the major problems in analysis of the solvent influence on the kinetics of electrode reactions is that a proper consideration of double-layer effects must be carried out. According to Frumkin theory, the observed rate constant, k_s , is related to the true value, k_{st} , by the following equation:²⁰

$$k_s = k_{st} \exp \left[\frac{(\alpha n - z) F \phi^r}{RT} \right] \quad (1)$$

where α is the transmission coefficient of the electrode process, ϕ^r is the potential at the reaction plane, and z is the charge of reactant. Therefore, consideration of the double-layer effect requires that one estimate the location of the reaction plane with respect to the outer Helmholtz plane (oHp) and the potential ϕ^r at this plane. The reaction plane is often thought to coincide with the oHp. Under this assumption, the ϕ^r potential is equal to the potential drop across the diffuse part of the double layer ϕ^d , which is related to the electrode surface charge density σ_m . The latter can be calculated from the charging current or by the integration of capacity-potential curves. For most electrode processes, the estimation of the influence of double-layer structure on the rate of electron transfer is a challenging task. First of all, the assumption that the reaction plane coincides with the oHp may not be valid. Additionally, particularly for solid electrodes and nonaqueous solutions, determination of the potential distribution profile across the double layer is extremely difficult. It has also been argued that the classical Gouy–Chapman–Stern theory, used for the ϕ^d potential calculation, tends to overestimate its value.²¹ To minimize the double-layer effect, most of the studies of solvent influence on heterogeneous electron transfer have involved redox couples in which the most

* Corresponding author. Fax: +1 530 7528995. E-mail: fawcett@indigo.ucdavis.edu.

[†] University of California.

[‡] University of Białystok.

[§] Present address: Department of Chemistry, University of West Indies, Mona, Jamaica.

highly charged species is a monovalent cation or anion. Since the oxidation of Ru(phen)_3^{2+} occurs at very positive potentials and the reactant in the electrode process has a double positive charge, it can be expected that the kinetics of charge transfer in this system would be strongly influenced by both double-layer structure and ion pair formation. Interestingly, Pyati and Murray,²² investigating the solvent dynamics effect on the heterogeneous electron-transfer rate constant of tris(2,2'-bipyridine)cobalt(II), did not observe strong double-layer or ion-pairing effects on the electrode reaction rate.

In the present paper, we report results of electron-transfer kinetics studies for the $\text{Ru(phen)}_3^{2+/3+}$ redox system. We focus primarily on examining the influence of double-layer structure and ion pair formation on the electrooxidation process. Our other aim is to investigate the effect of solvent on the rate of electrode reaction. The electrode behavior of the $\text{Ru(phen)}_3^{2+/3+}$ system is compared with the results reported recently^{22,23} for the $\text{Co(bpy)}_3^{2+/3+}$ redox couple.

Experimental Section

Reagents. Analytical grade solvents dimethylformamide (DMF), acetonitrile (AcN), butyronitrile (BuN), propylene carbonate (PC), dimethyl sulfoxide (DMSO), nitrobenzene (NB), and benzonitrile (BN) were dried over calcium hydride for 1 day and then distilled under reduced pressure. Tetra(*n*-butyl)-ammonium perchlorate (TBAP) (Sigma Chemical Co.) was dried under reduced pressure at 70 °C for 24 h. Tris(1,10-phenanthroline)ruthenium(II) perchlorate was prepared by a procedure proposed for tris(2,2'-bipyridine)ruthenium(II) perchlorate.²⁴

Electrochemical Measurements. All electrochemical measurements were performed using a three electrode system at 20 °C. A silver wire immersed in 0.01 M silver perchlorate and 0.09 M TBAP in acetonitrile and separated from the analyzed solution by a ceramic tip (Bioanalytical System Inc.) served as the reference electrode. The silver perchlorate solution was replaced daily because of the instability of Ag^+ to photoreduction. The stability of the reference electrode was examined by recording the ferrocene oxidation potential in the studied solvent as a function of time. The formal potential of the ferrocene/ferrocenium system was found to be stable for about 12 h. The counter electrode was made from platinum wire. The ultramicroelectrodes, which served as working electrodes in kinetic studies, were manufactured by sealing the metal wire (Goodfellow Metals Ltd., UK) into a soft glass capillary using a Bunsen burner flame. The capillary was then cut perpendicularly to its length, and the surface was polished using extra fine carborundum paper followed by 0.3 μm alumina. Electrical contacts were made using silver epoxy (Johnson Matthey Ltd., UK). In the determination of the $\text{Ru(phen)}_3^{2+/3+}$ formal potential and the diffusion coefficient of Ru(phen)_3^{2+} , a standard size gold disk electrode with a diameter of 1.5 mm (Bioanalytical System Inc.) was used as the working electrode. The solution was deaerated for 20 min with argon prior to electrochemical measurements.

Cyclic voltammetry was performed using an EG&G/PAR 273 potentiostat. The error in estimation of the formal potential was less than 5 mV. A Solatron 1250 frequency response analyzer served as the source of the dc potential and sinusoidal ac perturbation (10 mV peak-to-peak). The signal was fed into the external input of an EG&G/PAR 273 potentiostat through a low-impedance, purely resistive attenuator. The built-in current follower of the potentiostat was bypassed and replaced with a high-bandwidth (100 kHz) current preamplifier (EG&G Model 181). All instruments were connected to a common ground. The

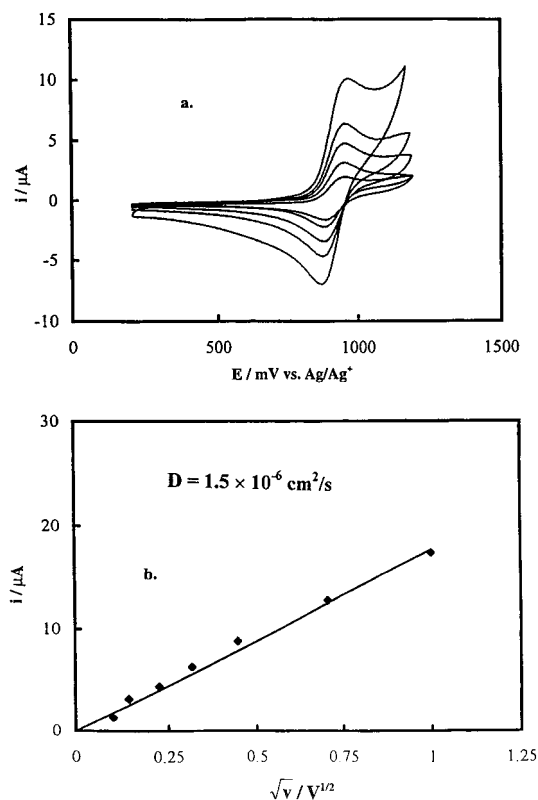


Figure 1. (a) Cyclic voltammograms of 1 mM Ru(phen)_3^{2+} oxidation in PC solution containing 0.1 M TBAP at a Au disk electrode (0.75-mm radius). The sweep rate was 20 (innermost), 50, 100, 200, and 500 mV s^{-1} (outermost). (b) The dependence of the oxidation peak current on the square root of sweep rate.

signal from the electrode was fed directly into this preamplifier. Its output and the reference signal from the potentiostat were fed into two channels of the frequency response analyzer to obtain the in- and out-of-phase components of the admittance.

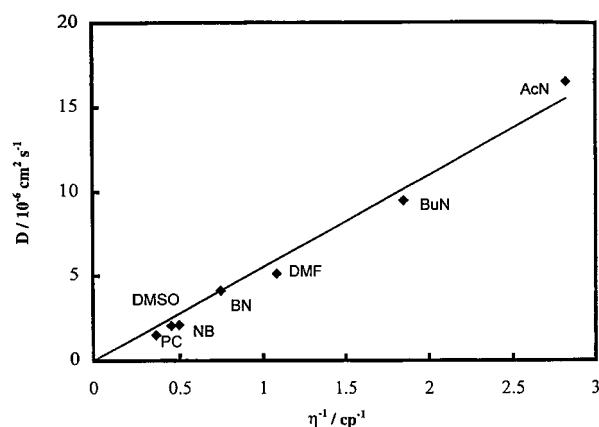
Results and Discussion

The process of Ru(phen)_3^{2+} electrooxidation was studied using standard size disk electrodes (0.75-mm radius) and ultramicroelectrodes by cyclic and ac-voltammetry. Typical cyclic voltammograms recorded in PC solution containing 0.1 M TBAP as a supporting electrolyte at the large electrode are presented in Figure 1a for different sweep rates. Similar curves were recorded for other solvents. The separation of peak potentials is equal to 58 mV and the ratio of anodic to cathodic peak currents close to one, confirming that the studied redox process is chemically and electrochemically reversible under dc conditions. From the slope of the expected linear relation between the cathodic peak current and the square root of the sweep rate (Figure 1b), the diffusion coefficient of the reactant (D) was calculated. The values of D obtained for different solvents are summarized in Table 1. A linear relationship between the diffusion coefficient and the reciprocal of solvent viscosity predicted by the Stokes–Einstein equation is presented in Figure 2. From the slope of this plot, an effective radius of Ru(phen)_3^{2+} equal to 0.42 nm was calculated. This value is somewhat smaller than the radius of Co(bpy)_3^{2+} obtained by Pyati and Murray.²²

The kinetics of electron transfer in the $\text{Ru(phen)}_3^{2+/3+}$ system was studied by ac-voltammetry. Admittance as a function of potential plots was obtained for different frequencies in the potential range of the faradaic process. Typical curves of in-

TABLE 1: Diffusion Coefficients of Ru(phen)₃²⁺, Observed Standard Rate Constants of Ru(phen)₃²⁺ Electrooxidation, and Outer-Sphere Gibbs Activation Energies in Different Solvents Containing 0.1 M TBAP

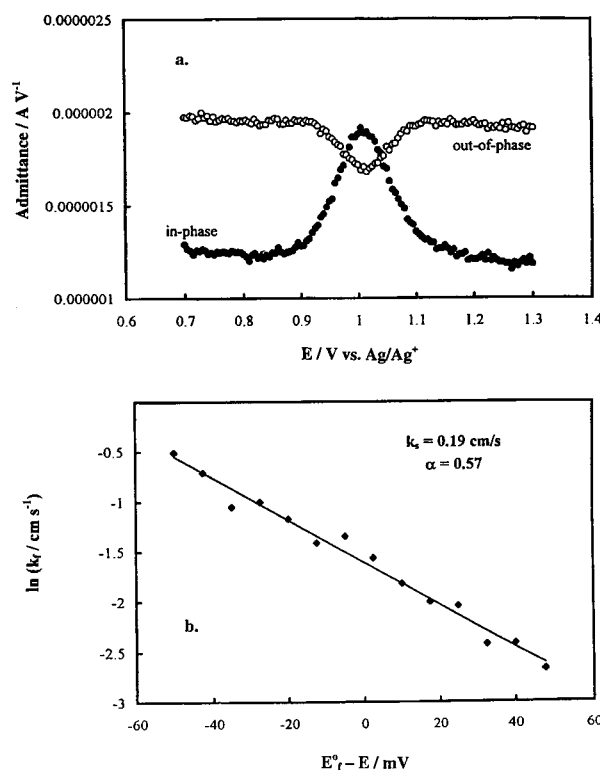
solvent	D cm ² s ⁻¹	k_s cm s ⁻¹	ΔG_{os}^* kJ mol ⁻¹
AcN	16.5×10^{-6}	1.7	22.1
BuN	9.3×10^{-6}	0.85	20.0
DMF	5.1×10^{-6}	0.47	19.4
BN	4.1×10^{-6}	0.53	16.3
DMSO	2.05×10^{-6}	0.26	18.3
NB	2.1×10^{-6}	0.16	16.2
PC	1.5×10^{-6}	0.22	20.1

**Figure 2.** Diffusion coefficient of Ru(phen)₃²⁺ in various solvents plotted against the reciprocal viscosity. 0.1 M TBAP was the supporting electrolyte.

and out-of-phase admittance as a function of potential for the electrooxidation of Ru(phen)₃²⁺ in PC obtained with a Au (25 μm) electrode are presented in Figure 3a. Nonfaradaic in-phase and out-of-phase admittance in the potential region preceding and following the faradaic peak were fitted to a third-order polynomial by least-squares, and then the polynomial expression was used to evaluate numerically the nonfaradaic components of the admittances in the peak region. The solution resistance and the double-layer capacitance were then calculated as a function of potential. For each experiment, the potential dependence of the activation resistance was obtained by a method previously described.²⁵ The forward rate constant k_f was calculated from the activation resistance R_a according to the equation:

$$k_f = \frac{RT}{2n^2 F^2 A R_{a,c_b}} \left[1 + \exp\left(-\frac{nF}{RT}(E - E_o^f)\right) \right] \quad (2)$$

where A is the electrode surface area, E is the dc potential of the working electrode, E_o^f is the formal potential of the redox system, and c_b is the bulk concentration of reactant. The formal potential of the Ru(phen)₃^{2+/3+} system was obtained by averaging the cathodic and anodic peak potentials of voltammograms recorded using the standard size gold electrode (Figure 1a). Figure 3b presents a typical plot of $\ln k_f$ as a function of overpotential ($E - E_o^f$). The standard rate constant and the electron-transfer coefficient were calculated from the intercept and the slope, respectively, using least-squares. The results of this analysis for different frequencies are collected in Table 2. In the studied frequency range, the kinetic parameters are almost independent of the frequency. After each experiment performed at constant frequency, the electrode was repolished. The constant value of double-layer capacitance at the formal potential of the Ru(phen)₃^{2+/3+} system suggests that the electrode surface is

**Figure 3.** (a) Plots of the in- and out-of-phase admittance as a function of potential for the oxidation of 1 mM Ru(phen)₃²⁺ in PC containing 0.1 M TBAP at the Au (25 μm) electrode. The frequency was 10 kHz. (b) Plot of the rate constant of Ru(phen)₃²⁺ oxidation in PC as a function of the overpotential.**TABLE 2: Results of Analysis of Admittance-Potential Plots for Different Frequencies, 0.1 mM Ru(phen)₃²⁺ in PC Containing 0.1 M TBAP**

frequency kHz	solution resistance kΩ	double layer capacitance μF cm ⁻²	α	k_s cm s ⁻¹
16	44.8	12.1	0.55	0.18
14	44.6	12.3	0.55	0.17
12	45.1	12.2	0.53	0.20
10	46.3	12.4	0.57	0.19
8	47.0	12.7	0.58	0.21
6	51.2	13.5	0.57	0.23
			$\bar{\alpha} = 0.56$	$\bar{k}_s = 0.20$

reproducible. At low frequencies, a dependence of solution resistance on frequency is observed. This effect was also reported for other systems studied at ultramicroelectrodes by ac voltammetry.²⁶ It is probably related to inaccurate sealing of the metal wire into glass so that the geometry of the working electrode cannot be represented as a perfectly inlaid disk.

The rate of the charge-transfer process in the studied system was also analyzed using the Randles method. From the plot of admittance as a function of potential, the in-phase and out-of-phase components of the faradaic impedance were calculated at the formal potential for different frequencies. Both the in-phase and out-of-phase components depend linearly on the reciprocal of the square root of the angular frequency ($\omega^{-1/2}$). This kind of plot obtained for Ru(phen)₃²⁺ electrooxidation in PC is shown in Figure 4. Good linear relations are observed. From the slope of both straight lines, the diffusion coefficient was calculated. The intercept of the plot of the real faradaic impedance against $\omega^{-1/2}$ is equal to the activation resistance at the formal potential. Therefore, using eq 2 the value of k_s can be calculated. In general, very good agreement between the

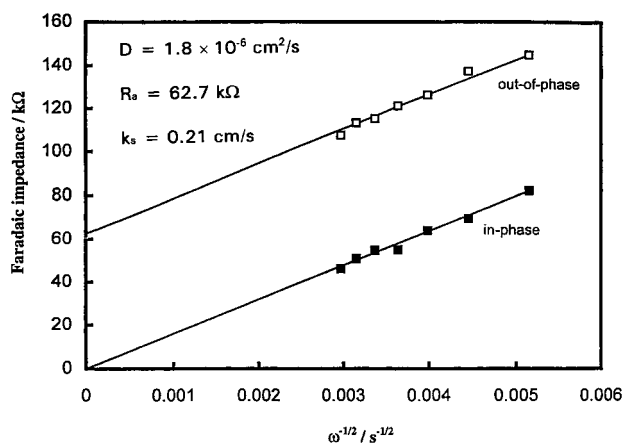


Figure 4. Plots of the in- and out-of-phase faradaic impedance measured at the formal potential of the $\text{Ru(phen)}_3^{2+/3+}$ system as a function of the reciprocal of the square root of angular frequency for the oxidation of 1 mM Ru(phen)_3^{2+} in PC containing 0.1 M TBAP at the Au (25 μm) electrode.

TABLE 3: Kinetic Parameters of Ru(phen)_3^{2+} Oxidation in AcN and PC at Au (25 μm) and Pt (12.5 μm) for Different Concentrations of Supporting Electrolyte

solvent	[TBAP] M	Au (25 μm)		Pt (12.5 μm)	
		α	$k_s \text{ cm s}^{-1}$	α	$k_s \text{ cm s}^{-1}$
PC	0.05	0.57	0.19		
	0.1	0.57	0.19	0.58	0.20
	0.2	0.56	0.20	0.57	0.22
	0.4	0.57	0.20	0.59	0.21
AcN	0.05	0.53	1.22	0.48	1.78
	0.1	0.56	1.39	0.50	1.62
	0.2	0.54	1.42	0.52	1.45
	0.4	0.52	1.35	0.52	1.50

standard rate constants obtained from the Tafel and Randles analyses was observed for all studied solvents.

To examine the double-layer effect, the influence of supporting electrolyte concentration and electrode material on the rate of electron transfer in the studied system were investigated. Equation 1 shows that the degree of double-layer effect on the electrode kinetics depends on the charge of the reactant, the potential range of the electrode reaction with respect to the potential of zero charge, and the location of reaction plane with respect to the outer Helmholtz plane (oHp). The fact that the $\text{Ru(phen)}_3^{2+/3+}$ system has a much more positive standard potential than the potential of zero charge of noble metal electrodes²⁷ and that the reactant has a double positive charge should lead to a significant influence of double-layer structure on the kinetics of charge transfer. In this study, both gold and platinum ultramicroelectrodes were used. For both electrodes, significant differences in the potential of zero charge have been reported.^{28–30} Since the ϕ^d potential depends on the concentration of supporting electrolyte, the rate constant should also depend on the TBAP concentration. The effect of supporting electrolyte concentration and electrode material on the standard rate constant of the $\text{Ru(phen)}_3^{2+/3+}$ system in PC and AcN solutions is presented in Table 3. As expected, the rate of electron exchange in AcN solution is higher than in PC, but almost no effect of TBAP concentration and electrode material was found in either solvent. A possible explanation is that the reaction plane is located outside of oHp, where the average potential is close to that in the bulk of solution. In the positive potential range, the oHp is formed by the centers of perchlorate anions, as shown in Figure 5. Recently, Fawcett³¹ estimated the Stokes radius of ClO_4^- in aprotic solvents. The radius of this

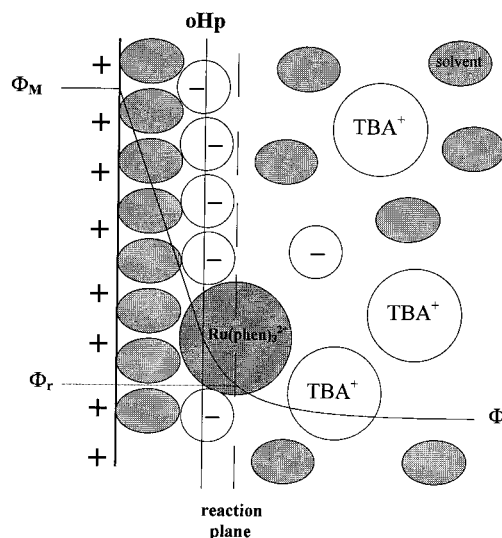


Figure 5. A schematic representation of the double-layer structure at the potentials of Ru(phen)_3^{2+} oxidation.

ion is more than two times smaller than the radius of Ru(phen)_3^{2+} . Therefore, it can be expected that the reaction plane for the oxidation reaction is shifted by about 2 nm toward the bulk of solution with respect to the oHp (Figure 5). The potential at the reaction plane may be close to that of the bulk of solution so that the studied system does not respond to the double-layer structure in the classical manner. Thus, we conclude that the obtained kinetic data do not require a double-layer correction. This is a great advantage in the present case because determination of interfacial parameters for these systems is very difficult. The results presented here indicate that $\text{Ru(phen)}_3^{2+/3+}$ is an excellent system for experimental investigation of different aspects of heterogeneous electron transfer.

The independence of the electrode reaction rate of the concentration of supporting electrolyte also indicates the absence of a strong ion pairing effect. The formation of ion pairs results in a change of the formal potential of the redox system and the effective concentration of the reactant in the solution. Both these factors should significantly affect the rate of charge transfer. However, the voltammetric study carried out in solution with varying concentrations of the supporting electrolyte indicates a very weak dependence of the formal potential on the supporting electrolyte concentration. Changes in the formal potential by 18 mV for NB and by 3 mV for PC for a 10-fold change in TBAP concentration were observed. These values indicate that ion pairing is probably not an important factor in the analysis presented in this paper.

The kinetics of Ru(phen)_3^{2+} oxidation was studied in seven aprotic solvents. The solvents were chosen for the study so that a relatively wide range of longitudinal relaxation times and outer-sphere Gibbs activation energies would be involved in our study of the solvent effect. The values of the standard rate constants and electron-transfer coefficients obtained in the different solvents and estimated values of the outer-sphere Gibbs activation energy are collected in Table 1. The values ΔG_{os}^* were calculated according to the Marcus model using a reactant radius of 0.42 nm and neglecting imaging.

In the preliminary analysis of kinetic data, it was assumed that the standard rate constant is expressed as

$$k_s = A\tau_L^{-\theta} \exp\left(-\frac{\Delta G_{os}^* + \Delta G_{is}^*}{RT}\right) \quad (3)$$

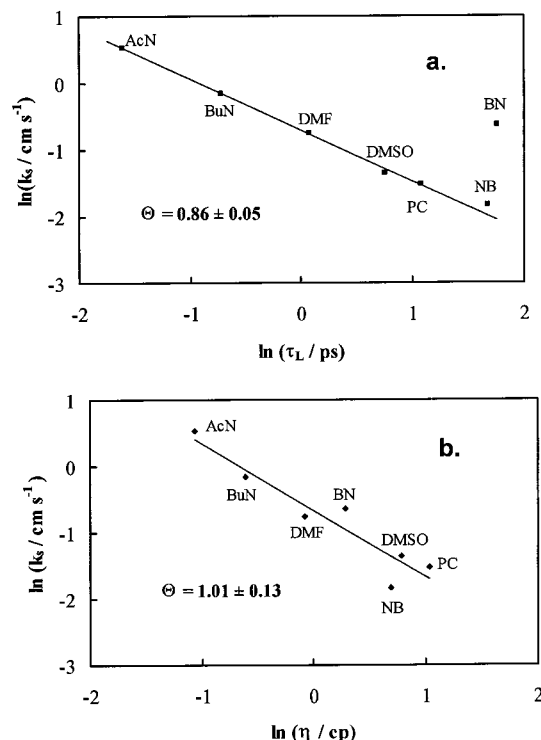


Figure 6. Plots of the logarithm of the standard rate constant, $\ln k_s$, for $\text{Ru}(\text{phen})_3^{2+}$ oxidation at the Au ($25\ \mu\text{m}$) electrode against the logarithm of the longitudinal relaxation time of solvent, $\ln \tau_L$, (a) and the logarithm of solvent viscosity, $\ln \eta$, (b).

where A is the portion of the preexponential factor that is approximately independent of the solvent, τ_L is the longitudinal relaxation time, θ is a fraction between 0 and 1 that depends on the degree of reaction adiabaticity, and ΔG_{os}^* and ΔG_{is}^* are the outer- and inner-sphere Gibbs activation energies, respectively. Assuming that the main contribution to the solvent effect comes from the longitudinal relaxation time, a linear relation between $\ln k_s$ and $\ln \tau_L$ with a slope equal to $-\theta$ should be observed. This plot for the process of $\text{Ru}(\text{phen})_3^{2+}$ electrooxidation is presented in Figure 6a. A relatively good linear correlation is observed. However, the value for θ obtained from the slope of this relation is significantly lower than unity. This probably reflects the fact that the influence of ΔG_{os}^* on the kinetics of charge transfer was not taken into account. The relationship between the viscosity and the Debye relaxation time indicates that the rate of the electrode process should also correlate with viscosity.³² This kind of correlation is presented in Figure 6b. A relatively good linear correlation with a slope close to 1 is observed. The values of θ obtained from plots of $\ln k_s$ against $\ln \tau_L$ and $\ln k_s$ against $\ln \eta$ point out that the studied process fulfills the criteria for adiabaticity.

For an adiabatic electron-transfer reaction, the constant A in eq 3 can be expressed by the following equation:

$$A = \kappa K_p \left(\frac{\Delta G_{\text{os}}^*}{4\pi RT} \right)^{1/2} \quad (4)$$

where κ is the electronic transmission coefficient and K_p , the encounter preequilibrium constant. It follows that eq 3 can be rewritten as:

$$\ln \frac{k_s}{\Delta G_{\text{os}}^{*1/2}} + \frac{\Delta G_{\text{os}}^*}{RT} = \ln \left[\frac{\kappa K_p}{(4\pi RT)^{1/2}} \right] - \frac{\Delta G_{\text{is}}^*}{RT} - \theta \ln \tau_L \quad (5)$$

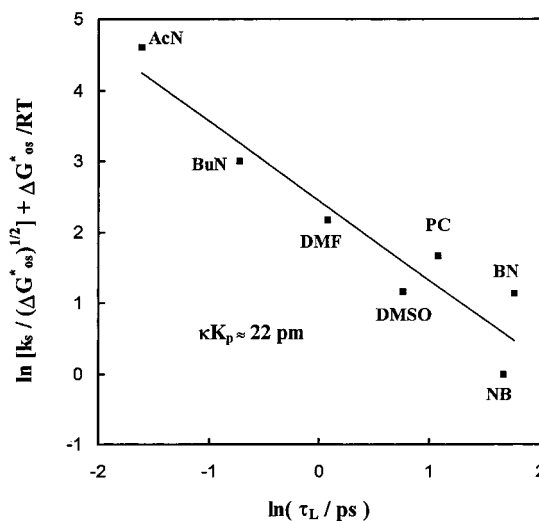


Figure 7. Plot of the corrected standard rate constant, $\ln [k_s / (\Delta G_{\text{os}}^*)^{1/2}] + \Delta G_{\text{os}}^* / RT$, for $\text{Ru}(\text{phen})_3^{2+}$ oxidation at the Au ($25\ \mu\text{m}$) electrode against the logarithm of the longitudinal relaxation time of solvent, $\ln \tau_L$.

This equation demonstrates that there should be a linear relationship between the left-hand side of the equation and $\ln \tau_L$. The relevant plot for the data of $\text{Ru}(\text{phen})_3^{2+}$ electrooxidation is shown in Figure 7. Analysis of the intercept allows one to estimate the parameter κK_p . Neglecting the inner-sphere activation energy, the estimate of κK_p is 20 pm. This value is only slightly lower than the one predicted by Hupp and Weaver.³³ For many other studied systems, analysis of the solvent effect leads to much lower values of the κK_p parameter.³⁴ Neglect of the double-layer effect is probably a major factor in the underestimation of this parameter.

Conclusions

The electron-transfer kinetics in the $\text{Ru}(\text{phen})_3^{2+/3+}$ system were studied in several aprotic solvents at gold and platinum ultramicroelectrodes. Similar to the behavior reported for the $\text{Co}(\text{bpy})_3^{2+/3+}$ system, no effect of the double layer on the kinetics of $\text{Ru}(\text{phen})_3^{2+}$ oxidation was observed. The standard rate constant is independent of the electrode material and the concentration of the supporting electrolyte. This behavior can be explained assuming that the reaction plane is located outside of the oHp. The difference in the size of the reactant and the ClO_4^- ions forming the oHp seems to confirm this explanation. Also, no significant influence of ion pair formation on the rate of the electron-transfer process is observed for the $\text{Ru}(\text{phen})_3^{2+/3+}$ system. Therefore, the process of $\text{Ru}(\text{phen})_3^{2+}$ oxidation can be very useful in the testing of the heterogeneous electron transfer theory. In addition, the $\text{Ru}(\text{phen})_3^{2+}$ complex approaches the apparent spherical geometry desirable for theoretical comparison.

Electron transfer for the $\text{Ru}(\text{phen})_3^{2+/3+}$ system is relatively fast. The standard rate constant changes from $1.7\ \text{cm s}^{-1}$ for AcN to $0.16\ \text{cm s}^{-1}$ for NB. The solvent effect on the rate of the electron transfer process can be successfully described on the basis of a dynamic effect on the preexponential factor. The studied electrode reaction is perfectly adiabatic.

The presented results demonstrate again that high-frequency ac admittance is a very powerful technique for the study of fast heterogeneous charge-transfer processes.

Acknowledgment. This work was supported by the National Science Foundation (Grant CHE-9729314).

References and Notes

- (1) Ghosh, B. K.; Chakravorty, A. *Coord. Chem. Rev.* **1989**, 95, 239.
- (2) Ohsawa, Y.; DeArmond, M. K.; Hanck, K. W.; Morris, D. E. *J. Am. Chem. Soc.* **1983**, 105, 6522.
- (3) Lever, A. B. P. *Inorg. Chem.* **1990**, 29, 1271.
- (4) Tokel-Takvoryan, N. E.; Hemingway, R. W.; Bard, A. J. *J. Am. Chem. Soc.* **1973**, 95, 6582.
- (5) Rillema, D. P.; Allen, G.; Meyer, T. J.; Conrad, D. *Inorg. Chem.* **1983**, 22, 1617.
- (6) Abruna, H. D. *Coord. Chem. Rev.* **1988**, 86, 135.
- (7) Calvert, J. M.; Meyer, T. J. *Inorg. Chem.* **1981**, 20, 27.
- (8) Denisevich, P.; Abruna, H. D.; Leidner, C. R.; Meyer, T. J.; Murray, R. W. *Inorg. Chem.* **1982**, 21, 2153.
- (9) Ellis, C. D.; Meyer, T. J. *Inorg. Chem.* **1984**, 23, 1748.
- (10) Hupp, J. T.; Otruba, J. P.; Pauris, S. J.; Meyer, T. J. *J. Electroanal. Chem.* **1985**, 190, 287.
- (11) Willman, K. W.; Murray, R. W. *J. Electroanal. Chem.* **1982**, 133, 211.
- (12) Samuels, G. J.; Meyer, T. J. *J. Am. Chem. Soc.* **1981**, 103, 27.
- (13) Pickup, G. P.; Kutner, W.; Leidner, C. R.; Murray, R. W. *J. Am. Chem. Soc.* **1984**, 106, 1991.
- (14) Beer, P. D. *J. Chem. Soc., Chem. Commun.* **1996**, 689.
- (15) Baxter, S. M.; Jones, W. E.; Danielson, E.; Worl, L. A.; Youthathan, J.; Strouse, G. F.; Meyer, T. J. *Coord. Chem. Rev.* **1991**, 111, 47.
- (16) Geraty, S.; Vos, J. G. *J. Electroanal. Chem.* **1984**, 176, 389.
- (17) Margerum, L. D.; Meyer, T. J.; Murray, R. W. *J. Electroanal. Chem.* **1983**, 149, 279.
- (18) Maggini, M.; Guldi, D. M.; Mondini, S.; Scorrano, G.; Paolucci, F.; Ceroni, P.; Roffia, S. *Chem. Eur. J.* **1998**, 4, 1992.
- (19) Saji, T.; Aoyagui, S. *J. Electroanal. Chem.* **1975**, 63, 31.
- (20) Frumkin, A. N. *Z. Phys. Chem.* **1933**, 164, 121.
- (21) Mohilner, D. M. In *Electroanalytical Chemistry*; Bard, A. J., Ed.; Marcel Dekker: New York, 1966; Vol. 1, Chapter 3.
- (22) Pyati, R.; Murray, R. W. *J. Am. Chem. Soc.* **1996**, 118, 1743.
- (23) Williams, M. E.; Crooker, J. C.; Pyati, R.; Lyons, L. J.; Murray, R. W. *J. Am. Chem. Soc.* **1997**, 119, 10249.
- (24) Burstall, F. H.; Nyholm, R. S. *J. Chem. Soc.* **1952**, 3570.
- (25) Baranski, A. S. *J. Electroanal. Chem.* **1991**, 300, 309.
- (26) Winkler, K.; Baranski, A. S.; Fawcett, W. R. *J. Chem. Soc., Faraday Trans.* **1996**, 92, 3899.
- (27) Frumkin, A. N.; Petri, O. A.; Damaskin, B. B. In *Comprehensive Treatise of Electrochemistry*; Bockris, J. O'M., Conway, B. E., Yeager, E., Eds.; Plenum: New York, 1984; Vol 1.
- (28) Petrii, O. A.; Khomchenko, I. G. *J. Electroanal. Chem.* **1980**, 106, 277.
- (29) Marinkovic, N. S.; Hecht, M.; Loring, J. S.; Fawcett, W. R. *Electrochim. Acta* **1996**, 41, 641.
- (30) Hamelin, A.; Doubova, L.; Wagner, D.; Schrimmer, H. J. *Electroanal. Chem.* **1987**, 220, 155.
- (31) Fawcett, W. R. *Mol. Phys.* **1998**, 95, 507.
- (32) Davies, M. In *Dielectric Properties and Molecular Behavior*; Hill, N. E., Waughan, W. E., Price, A. H., Davies, M., Eds.; Van Nostrand Reinhold: London, 1969; Chapter 5.
- (33) Hupp, J. T.; Weaver, M. J. *J. Phys. Chem.* **1984**, 88, 1467.
- (34) Fawcett, W. R.; Foss, C. A. J., Jr. *Electroanal. Chem.* **1989**, 270, 103.